Brevican-deficient mice display impaired hippocampal CA1 long-term potentiation but show no obvious deficits in learning and memory

Brakebusch, Cord; Seidenbecher, Constanze I.; Asztély, Fredrik; Rauch, Uwe; Matthies, Henry; Meyer, Hannelore; Krug, Manfred; Böckers, Tobias M.; Zhou, Xiaohong; Kreutz, Michael R.; Montag, Dirk; Gundelfinger, Eckart D.; Fässler, Reinhard

Published in:
Molecular and Cellular Biology

DOI:
10.1128/MCB.22.21.7417-7427.2002

2002

MOLECULAR AND CELLULAR BIOLOGY, Nov. 2002, p. 7417–7427 Vol. 22, No. 21
0270-7306/02/$04.00+0 DOI: 10.1128/MCB.22.21.7417–7427.2002

Brevican-Deficient Mice Display Impaired Hippocampal CA1 Long-Term Potentiation but Show No Obvious Deficits in Learning and Memory

Cord Brakebusch,[1,2] Constanze I. Seidenbecher,[3] Fredrik Asztely,[4] Uwe Rauch,[2] Henry Matthies,[3] Hannelore Meyer,[1] Manfred Krug,[3] Tobias M. Böckers,[5] Xiaohong Zhou,[2] Michael R. Kreutz,[3] Dirk Montag,[6] Eckart D. Gundelfinger,[3] and Reinhard Fässler[1,2]*

Department of Molecular Medicine, Max Planck Institute of Biochemistry, 82152 Martinsried,[1] Department of Neurochemistry and Molecular Biology[3] and Neurogenetics Research Group,[6] Leibniz Institute for Neurobiology, 39118 Magdeburg, and Institute for Anatomy, University of Münster, 48149 Münster,[5] Germany, and Department of Experimental Pathology[2] and Department of Neurology,[4] Lund University Hospital, 22185 Lund, Sweden

Received 17 April 2002/Returned for modification 10 June 2002/Accepted 16 July 2002

Brevican is a brain-specific proteoglycan which is found in specialized extracellular matrix structures called perineuronal nets. Brevican increases the invasiveness of glioma cells in vivo and has been suggested to play a role in central nervous system fiber tract development. To study the role of brevican in the development and function of the brain, we generated mice lacking a functional brevican gene. These mice are viable and fertile and have a normal life span. Brain anatomy was normal, although alterations in the expression of neurocan were detected. Perineuronal nets formed but appeared to be less prominent in mutant than in wild-type mice. Brevican-deficient mice showed significant deficits in the maintenance of hippocampal long-term potentiation (LTP). However, no obvious impairment of excitatory and inhibitory synaptic transmission was found, suggesting a complex cause for the LTP defect. Detailed behavioral analysis revealed no statistically significant deficits in learning and memory. These data indicate that brevican is not crucial for brain development but has restricted structural and functional roles.

During development the brain extracellular matrix (ECM) is suggested to play a role in cell adhesion, cell migration, and axon guidance (38). In the adult brain the ECM might stabilize established neuronal connections and determine the mature neural plasticity of the central nervous system (CNS) (41). In contrast to the ECM of other tissues, it is rich in proteoglycans, hyaluronic acid, and tenascins but lacks molecules such as fibrillar collagens and fibronectin (24). Lecticans are an important family of proteoglycans. Family members aggrecan, neurocan, brevican, and versican are found in the brain (43). Lecticans are characterized by a C-terminal C-type lectin domain, an N-terminal hyaluronan binding domain, and a highly diverse central domain with attached glycosaminoglycan side chains and other poly- and oligosaccharides. The C-terminal domain of brevican interacts strongly with the glycoprotein tenascin R in a calcium-dependent manner (1). In addition, it binds to cell surface sulfatides and sulfoglucuronyl glycolipids (SGGLs), which may act as cell surface receptors for brevican. The central domain of brevican contains three potential glycosaminoglycan attachment sites. In the adult brain, brevican is found as a chondroitin sulfate proteoglycan but also as a glycoprotein without any glycosaminoglycan attachments (17). Brevican occurs as a secreted molecule and in a C-terminally truncated glycosylphosphatidylinositol-anchored form (33). Like the other lecticans, brevican is also proteolytically cleaved, giving rise to a 50-kDa N-terminal fragment and a 90-kDa fragment (42). Brevican expression in the mouse starts at embryonic day 14 and increases significantly after birth, reaching a plateau around 150 days after birth (U. Rauch and R. Fässler, unpublished data).

Chondroitin sulfates are found in "barriers" against cell migration and axon growth in vivo. In vitro, chondroitin sulfate-carrying lecticans inhibit neurite outgrowth (22). Since neurite outgrowth is promoted by the nonproteoglycan form of brevican, it has been suggested that regulation of the attachment of the chondroitin sulfate side chain to brevican might be important for the modulation of axon growth (18). Both brevican and its binding partner tenascin R are deposited around cell bodies and proximal dendrites of large nerve cells, contributing to a "perineuronal net" (PNN) consisting of lecticans, hyaluronan, and tenascin R (9). This PNN has been suggested to be a repulsive barrier against approaching axons and dendrites, thus preventing the formation of new synapses. In vivo experiments have indicated an important role for the hyaluronan-binding N-terminal fragment of brevican in the modulation of cell migration, since glioma cells overexpressing it displayed increased invasiveness (25).

To understand the role of brevican during development and in the adult brain, we generated and analyzed mice lacking a functional brevican gene. It was of particular interest to compare these mice with neurocan-deficient mice (45). Neurocan is the closest relative of brevican. It also shows neural-tissue-

* Corresponding author. Mailing address: Department of Molecular Medicine, Max Planck Institute of Biochemistry, Am Klopferspitz 18A, 82152 Martinsried, Germany. Phone.: 49-89-8578 2897. Fax: 49-89-8578 2422. E-mail: faessler@biochem.mpg.de.

specific expression, but in contrast to that of brevican, which is one of the most prominent proteoglycans in the adult brain, neurocan expression peaks earlier in development and declines in the mature CNS (45). Therefore, the mature brain was expected to be more severely affected in brevican-deficient mice.

MATERIALS AND METHODS

Generation of brevican-deficient mice. The targeting construct to inactivate the brevican gene was made by using a cosmid clone of the mouse brevican gene described previously (29). A promoterless *lacZ* gene and a neomycin resistance expression cassette under the control of the phosphoglycerate kinase (PGK) promoter were flanked by a 2.5-kb *Sal*I-*Not*I fragment and a 5.2-kb *Xho*I-*Nsi*I fragment, thus introducing the *lacZ* gene, after homologous recombination, into exon 2, carrying the 5′untranslated region, and deleting the complete coding and 3′ noncoding part. The construct was linearized and electroporated into R1 embryonic stem cells as described previously (7). After selection for stable transfectants, homologous recombinants were identified by digestion of genomic DNA with *Eco*RI and Southern blot analysis using a 0.9-kb *Hin*dIII-*Nco*I fragment of the 5′ upstream region of the brevican gene as an external probe. Two clones were then injected into C57BL/6 blastocysts, and injected blastocysts were transferred into pseudopregnant foster mothers. Both clones gave germ line transmission and were used for establishing 129Sv inbred and 129Sv × C57BL6 outbred lines. For behavioral studies, mice were backcrossed for at least 5 generations to strain C57BL/6, including 1 generation using a C57BL/6 male, and then intercrossed to obtain homozygous brevican-deficient mice.

Immunofluorescence. Brains from 10- and 30-day-old mice were frozen in optimal cutting temperature compound (OCT) and cut into thin (5-μm) sections. Sections were fixed with 4% paraformaldehyde and stained by using standard protocols. The following rabbit antibodies were used: anti-brevican, anti-neurocan, anti-tenascin C (all kindly provided by R. Timpl, Martinsried, Germany), and anti-tenascin R (kindly provided by A. Aspberg, Lund, Sweden). Cy3-conjugated donkey anti-rabbit immunoglobulin G (IgG) (Jackson Immunoresearch) was used as a secondary antibody.

Northern blotting. Total RNA was isolated from adult brains as described by Auffray and Rougeon (2). Northern blotting was carried out by following standard protocols. For hybridization, fragments of mouse neurocan cDNA (nucleotides 30 to 730), mouse brevican cDNA (nucleotides 2160 to 2450), mouse tenascin C cDNA (1,340-bp *Apa*I/*Hin*dIII fragment), mouse tenascin R cDNA, and mouse glyceraldehyde-3-phosphate dehydrogenase cDNA were used.

Western blotting. For analysis of mutant mice, rabbit antisera raised against rat brain-derived and recombinant (for booster injections) rat neurocan, against recombinant rat brevican, against recombinant mouse tenascin C (all kindly provided by R. Timpl), and against tenascin R (kindly provided by A. Aspberg) were used. Briefly, mouse brains were homogenized in 5 volumes of 20 mM Tris-HCl (pH 8.0)–150 mM NaCl–5 mM EDTA–5 mM benzamidine–5 mM *N*-ethylmaleimide–1 mM phenylmethylsulfonyl fluoride. After 15 min of centrifugation at 10,000 × *g*, Triton X-100 was added to the supernatant to a final concentration of 0.5%. For analysis of the soluble brain fraction, all soluble molecules (i.e., molecules not sedimented after 10 min at 15,000 × *g*) were adjusted to 30 mM sodium acetate–100 mM Tris-Cl (pH 8.0) and treated with 1 mU of protease-free chondroitinase ABC/15 μl (≈30 μg of protein) for 45 min at 37°C. Samples were suspended in nonreducing sodium dodecyl sulfate (SDS) sample buffer and analyzed for their protein content. Thirty micrograms of protein was applied per lane for SDS-polyacrylamide gel electrophoresis (PAGE) analysis. Whole-brain lysates were sonicated twice for 20 s each time, suspended in nonreducing SDS sample buffer, and analyzed for their protein content. Fifty micrograms of protein was applied per lane for SDS-PAGE analysis under reducing conditions. SDS-PAGE and Western blotting on polyvinylidene difluoride membranes with peroxidase-conjugated secondary antibodies and an enhanced-chemiluminescence substrate were performed according to standard protocols. For total-brain lysates, equal protein loading was controlled by probing with antibodies against neurofilament M (Chemicon, Temecula, Calif.).

Electron microscopy. For electron microscopy, mice were perfused with Karnovsky's solution (2.2% glutaraldehyde and 2.5% paraformaldehyde in 0.1 M phosphate buffer [pH 7.35]). Brains were dissected and cut on a Vibratome (200-μm sections) in a sagittal orientation. Sections were incubated for 24 h at 4°C with biotinylated *Wisteria floribunda* agglutinin. The staining was developed with ABC reagent (Vector Laboratories, Burlingame, Calif.) and enhanced with diaminobenzidine and silver as described previously (3). Subsequently, the hippocampal CA1 region was carefully removed, postfixed in 1% OsO_4, dehydrated in alcohol, and embedded in Epon. Ultrathin sections were contrasted with uranyl acetate and lead citrate and were examined with a Philips electron microscope.

Electrophysiology. Electrophysiological recordings in the CA1 regions of the hippocampi of adult male mice were performed as described previously (45). Briefly, 400-μm transverse hippocampal slices were superfused with artificial cerebrospinal fluid (aCSF, comprising 119 mM NaCl, 2.5 mM KCl, 1.3 mM $MgSO_4$, 2.5 mM $CaCl_2$, 26.2 mM $NaHCO_3$, 1 mM NaH_2PO_4, and 11 mM glucose), saturated with 95% O_2–5% CO_2, and kept at 35°C. For recording of the field excitatory postsynaptic potential slope (fEPSP), glass recording electrodes were filled with aCSF and inserted into the basal dendritic layer of the CA1 region. Long-term potentiation (LTP) was induced by tetanization of the Schaffer collaterals with three 100-Hz stimulus series, each containing 50 pulses of 0.4-ms pulse width, with a 5-min-interval between the series. In order to monitor the time course of LTP, test potentials were recorded every 5 to 10 min until 5 h after tetanization. For comparison, rabbit anti-brevican antibodies (33) were used to interfere with brevican function in hippocampal slices from Wistar rats by following the protocol described previously (34). Briefly, IgG fractions from antisera were affinity purified on GammaBind Plus Sepharose (Pharmacia) and buffer exchanged into aCSF on fast protein liquid chromatography fast-desalting columns (Pharmacia). Antibodies at 1 mg/ml were then applied to the CA1 stratum radiatum by using a microinfusion pump (delivery rate, ~0.75 μl/min). After 60 min of antibody infusion, LTP was induced. In control experiments a normal rabbit IgG fraction was applied at the same concentration to assess nonspecific protein effects.

For patch-clamp recordings of excitatory synaptic transmission, brain slices were transferred to the recording chamber and submerged in aCSF with 100 μM picrotoxin added to block GABA(A) receptor-mediated responses. The temperature was kept between 21 and 23°C. The Schaffer collaterals were stimulated with isolated bipolar stainless steel electrodes at 0.2 Hz. Interstimulus intervals (ISI) for paired pulses were 25, 50, and 200 ms. Whole-cell recording pipettes (4 to 5 MΩ) were filled with 97.5 mM Cs gluconate, 17.5 mM CsCl, 10 mM HEPES, 5 mM BAPTA (Molecular Probes, Eugene, Oreg.), 8 mM NaCl, 2 mM MgATP, 0.3 mM GTP, and 5 mM QX-314 Br (pH 7.2; osmolarity, 295 mOsm). Membrane currents were amplified and filtered at 2.98 kHz, sampled at 10 kHz with an EPC-9 patch-clamp amplifier (HEKA Electronics, Lambrecht, Germany), and stored on a Power Macintosh for offline analysis. The series resistance was continuously monitored by delivering a voltage command at the end of each trace recorded. A liquid junction potential of −13 mV was calculated between the intracellular and extracellular solution with the generalized Henderson liquid junction potential equation.

For recordings of inhibitory synaptic transmission, the slices were transferred to the recording chamber and submerged in aCSF to which 5 μM 6-nitro-7-sulfamobylbenzo(f)quinoxaline-2,3-dione (NBQX) and 1 μM 3-(*R*)-2-carboxypiperazin-4-yl)-propyl-1-phosphonic acid (CPP) had been added to block α-amino-3-hydroxy-5-methyl-4-isoxalone propionic acid (AMPA) and *N*-methyl-D-aspartate (NMDA) receptor-mediated responses. In experiments recording spontaneous inhibitory postsynaptic currents (sIPSCs), the temperature was kept between 29 and 31°C to increase the frequency of sIPSCs. Pipettes were filled with 135 mM CsCl, 10 mM HEPES, 0.2 mM EGTA, 8 mM NaCl, 2 mM MgATP, 0.3 mM GTP, and 5 mM QX-314 Br (pH 7.2; osmolarity, 295 mOsm). Junction potentials were not compensated, but the reversal potential of the evoked and spontaneous IPSCs were routinely measured and fell close to the calculated Cl^- equilibrium potential. Addition of 100 mM picrotoxin abolished all the IPSCs in both mutant and control mice. Statistical analysis was carried out with the two-tailed Mann-Whitney U test. Results are shown as percent deviation of the actual records from baseline ± standard error of the mean (SEM).

Behavioral paradigms. For all behavioral experiments, brevican-deficient mice and matched wild-type littermates derived from heterozygous matings were tested by an experimenter unaware of the genotype. Eleven brevican-deficient and 10 wild-type mice were subjected to a series of tests conducted in the following order: determination of home cage activity and of food and water consumption, examination of general behavior and neurological state, grip strength, open field, four-hole board, elevated plus maze, light-dark avoidance, rota-rod, and water maze. A different group of eight mutant mice and eight littermate controls was analyzed in the shuttle box paradigm.

(i) General behavior and neurological state. General parameters indicative of health and neurological state were obtained by conducting a neurobehavioral examination (appearance, sensorimotor behavior, immobility, and the animal's reflexes) as described by Wishaw et al. (39). In addition, the tests described in the primary screen of the SHIRPA protocol, except for the startle response, were

conducted (30; available from www.mgc.har.mrc.ac.uk/mutabase/shirpa_summary.html).

(ii) Analysis of home cage behavior. Animals had ad libidum access to water and food and were housed individually. Activity patterns were determined by using motility platforms (TSE, Bad Homburg, Germany) registering vibrations. Vibrations during 1-min periods were summed, registered, and used to construct a 24-h activity profile. Simultaneously, amounts of drinking-water and food consumption were determined over a 24-h period by use of a drinking and feeding monitoring system (TSE).

(iii) Grip strength measurement. Forelimb grip strength was measured (15) with a high-precision force sensor (Grip Strength Meter; TSE) for each animal in five trials. The maximal grip strength displayed by each animal was used for comparison of groups and statistical analysis.

(iv) Rota-rod. An accelerating rota-rod (TSE) was used to analyze motor coordination (11). Mice were subjected to two training sessions (intertrial interval, 3 h) with speed accelerating from 4 to 40 rpm over a 5-min period on the first day. After 3 days of rest, animals were tested at constant speeds of 16, 24, 32, and 40 rpm, with trials lasting 5 min at most. The time animals were able to maintain their balance on the rod was measured.

(v) Open field. The open-field test was performed in a square grey plastic arena (area, 50 cm^2, height, 25 cm; ca. 200 lx). Animals were placed in the middle of the arena, and their behavior was videotaped for 15 min. For evaluation, tracks were recorded by using the VideoMot 2 system (TSE), and path length, relative time, visits, and walking speed in the central area (infield; 30 cm^2), in the area closer to the walls (within 10 cm; outfield), and in the four corners (10 cm^2 each) of the arena were analyzed for the total test time (15 min) and for each 5-min interval. In addition, tracks were evaluated with Wintrack analysis software (36).

(vi) Four-hole board. An additional floor plate containing four holes (diameter, 2 cm; depth, 3 cm; black walls and floor) was inserted into a box like that used for the open-field test. During a 15-min session, the number of holes investigated, the time spent for these investigations, whether uprighting took place with or without wall contact, whether cleaning took place in the vicinity of the wall or distant from it, and the number of fecal boli were determined.

(vii) Light-dark avoidance. Light-dark avoidance (5, 6) was analyzed in a rectangular grey plastic arena with a dark (12.5 by 25 cm) and an illuminated (25 cm^2) compartment separated by a wall with a 5-cm^2 opening (35). Animals were placed in the middle of the illuminated compartment (ca. 250 lx), and their behavior was videotaped for 10 min. For analysis, the time spent in the dark versus the illuminated area, the number of transitions between the compartments, the duration of stays, and latency before entry into the dark compartment were compared.

(viii) Elevated plus maze. Animals were placed in the center of an elevated plus maze (13, 28) (arms, 6.5 by 45 cm; 75 cm above floor level; 22-cm-high nontransparent side walls), and their behavior over 5 min was recorded on videotape. The number of entries into the central part or the closed or open arms and the time spent in these compartments were registered, and path lengths were analyzed by using the VideoMot 2 system (TSE).

(ix) Morris water maze. The water maze (20) consisted of a dark-grey circular basin (diameter, 130 cm) filled with water (24 to 26°C; depth, 30 cm) made opaque by the addition of white paint. A circular platform (diameter, 10 cm) was placed 1.5 cm below the water surface. Mice were submitted to six trials per day for 6 days. They were allowed to swim until they found the platform or 120 s had elapsed. In the latter case, animals were guided to the platform and allowed to rest for 10 s. The hidden platform remained at a fixed position for the first 4 days (24 trials; acquisition phase) and was moved into the opposite quadrant for the last 2 days (12 trials; reversal phase). Trials 25 and 26 were defined as probe trials to analyze the precision of spatial learning. All trials were videotaped and analyzed by using the VideoMot 2 system (TSE) and Wintrack analysis software (40).

(x) Active avoidance. Active-avoidance learning was analyzed in the shuttle box paradigm by using standard equipment (TSE). Animals were examined for 5 days with one training session per day, consisting of 80 trials (10 s of conditioned stimulus [CS] [light] followed by 5 s of unconditioned stimulus [UCS] [0.3 mA pulsed]), and a 5- to 15-s intertrial interval that was varied stochastically. The numbers of active-avoidance reactions for the two groups were compared.

Statistical analysis. Statistical analysis was performed by using analysis of variance (one-way, two-way, or repeated-measures analysis of variance as appropriate) and the Statview program (SAS Institute Inc., Cary, N.C.). Comparisons of means were used as a posthoc test (Fisher's protected least significant difference with Bonferroni's and Dunn's correction). A P value of <0.05 was considered significant.

RESULTS

Generation of brevican-deficient mice. Brevican-deficient mice were generated by introducing a *lacZ* gene into exon 2 and deleting the entire coding region of the brevican gene (Fig. 1A and B). These mice showed no detectable levels of brevican mRNA (Fig. 1C) or protein (data not shown) as tested by Northern and Western blotting. Heterozygous mating produced offspring at a normal Mendelian ratio, indicating no embryonic lethality of homozygous mutants. Brevican-null mice were viable and fertile and had a normal life span. No difference in phenotype was observed between 129Sv inbred and C57BL/6 $\times$ 129Sv outbred mutant mice.

Morphology of mutant brains and expression of brevican-related and -interacting proteins. To assess brain morphology, Nissl staining and hematoxylin-and-eosin staining of brain sections derived from 10- and 30-day-old mice were carried out. No obvious difference was detected between brevican-deficient and wild-type animals (data not shown). Although brevican is ubiquitously expressed in the brain, expression levels are highest in the cerebellum, which also shows a rather remarkable spatial organization of brevican deposition. Furthermore, brevican expression coincides with the maturation of cerebellar glomeruli, and purified brevican inhibits neurite outgrowth of cerebellar granule neurons (42). It has therefore been suggested that brevican may play a crucial role in the maturation of the mossy fiber system in the cerebellum (42). To check whether the loss of brevican in the cerebellum is compensated for by increased production of neurocan or accompanied by changes in expression or deposition of the brevican binding protein tenascin R or the neurocan binding protein tenascin C (8), we analyzed the expression of these proteins by immunofluorescence. Neurocan and tenascin R were similarly expressed in mutant and control mice (Fig. 1D). However, tenascin C immunoreactivity appeared to be less prominent in the granule cell layers of 30-day-old brevican-null mice than in those of wild-type mice (Fig. 1D). Brains of 10-day-old mutant and control mice showed no difference.

In contrast to the cerebellum, neurocan appeared to be up-regulated in the forebrain as detected by immunofluorescence (data not shown). Therefore, we performed quantitative Western blot analyses of the soluble brain fraction and of whole-brain lysates. They confirmed an up-regulation of neurocan protein in the brains of 30-day-old mutant mice compared to control mice, whereas the levels of tenascin C and tenascin R were unchanged (Fig. 2 and data not shown). Densitometric quantification showed that in the soluble brain fractions of 30-day-old brevican-null mice, neurocan was significantly up-regulated, by about 65%. Analysis of total-brain lysates revealed a 70% $\pm$ 27% increase in the deposition of neurocan in mutant mice (three mutants and three controls were tested). No clear change was observed in 10-day-old mice (data not shown). Proteolytic processing of neurocan was not affected by the loss of brevican, as is visible in samples treated with chondroitinase ABC (Fig. 2).

Due to its repulsive properties and its presence in PNN, brevican has been suggested to be important for the maturation and stabilization of the neuronal network by preventing the formation of new synapses (9). To test this hypothesis, we carried out an ultrastructural investigation of the hippocampal

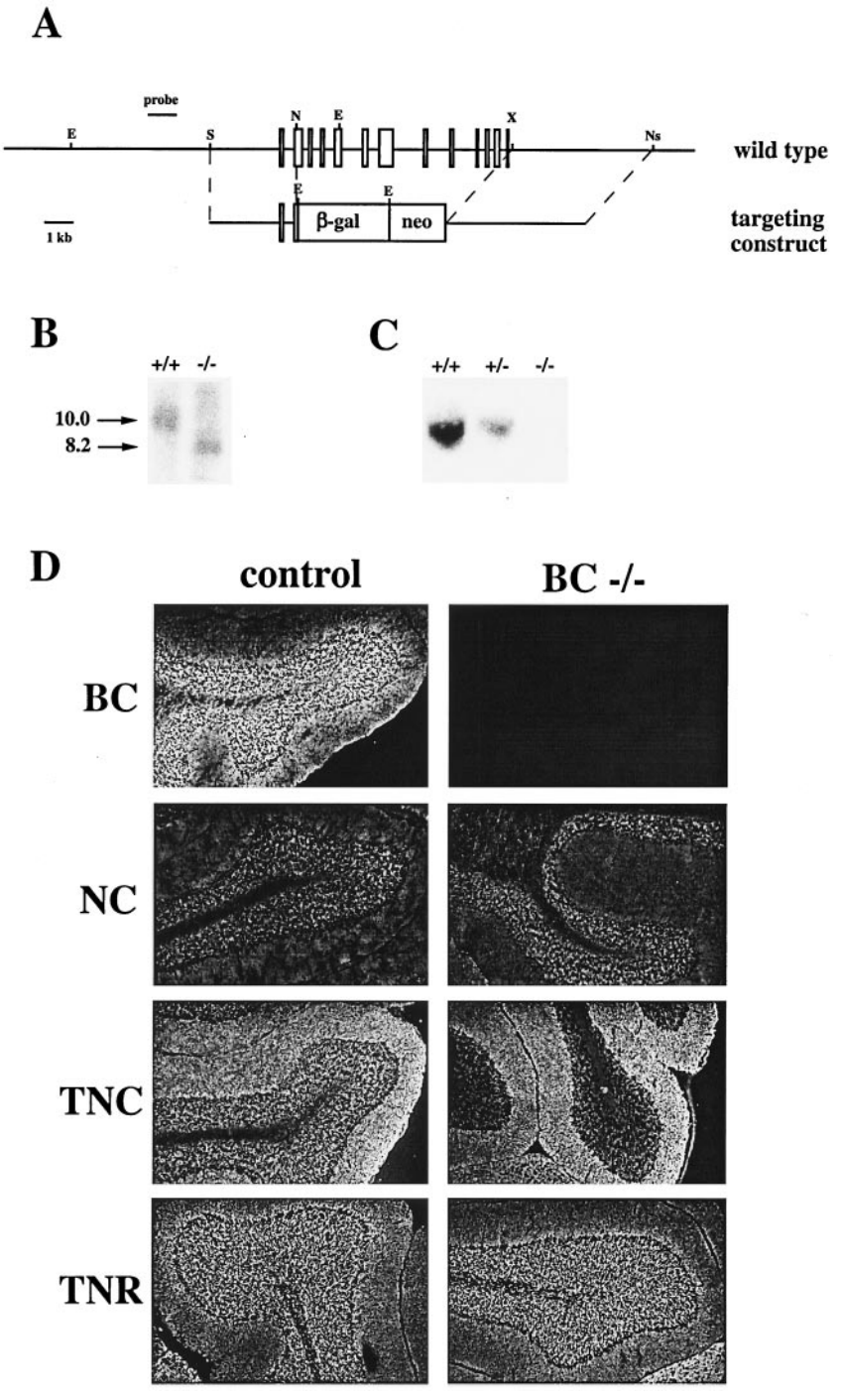

FIG. 1. Generation of brevican-null mice. (A) Targeting strategy. Exons are indicated by boxes. E, *Eco*RI; S, *Sal*I; N, *Not*I; Ns, *Nsi*I. (B) Southern blot detection of homozygous brevican-mutant mice. (C) Northern blotting for brevican using total RNA in wild-type (+/+), heterozygous (+/−), and homozygous (−/−) brevican-mutant mice. Size, approximately 3.4 kb. (D) Expression of brevican, neurocan, tenascin C, and tenascin R in the cerebellum. Cryosections of cerebella of mutant and normal mice were stained with antibodies against brevican, neurocan, tenascin C, and tenascin R and a secondary antibody conjugated to Cy3. BC, brevican; NC, neurocan; TNC, tenascin C; TNR, tenascin R.

CA1 region, which contains the physiologically best characterized synapses in the brain. However, mutant mice revealed no alterations (Fig. 3). Both the frequency and the size and structure of excitatory synapses appeared unaffected. Staining for PNNs, specialized ECM structures found around large brain neurons, with *W. floribunda* lectin showed slightly reduced staining in the brevican-null mice (Fig. 3A through D). The general structure of the PNNs, however, seemed to be unaltered. Interestingly, the PNNs appeared less stringent and concentrated at the plasma

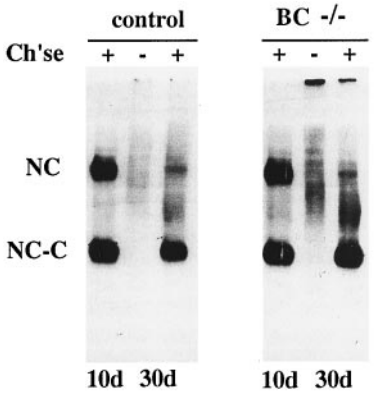

FIG. 2. Increased expression of neurocan in soluble brain extracts of brevican-deficient and normal mice. Western blot analysis was carried out on 30 μg of soluble brain extracts from 10- and 30-day-old brevican-null and control mice by using polyclonal antibodies against neurocan. Before separation on an SDS-PAGE gel, samples were either treated with chondroitinase ABC (Ch'se) or left untreated. The antibody detects full-length neurocan (NC) and the C-terminal proteolytic fragment of neurocan (NC-C).

membrane but more diffuse and dispersed, as demonstrated in the ultrastructural images.

Normal basic properties of excitatory and inhibitory synaptic transmission. To investigate synaptic function in mutant mice, basal properties and short-term plasticity of excitatory and inhibitory synapses to the pyramidal cells in the hippocampal CA1 region were studied. We first analyzed the basal excitatory synaptic transmission at Schaffer collateral–pyramidal-cell synapses in the hippocampal CA1 region in the presence of the GABA(A) receptor antagonist picrotoxin to block fast inhibitory synaptic transmission. The gross pharmacological properties of AMPA receptor (cell clamped at −70 mV)- and NMDA receptor (cell clamped at +40 mV in the presence of the AMPA receptor antagonist NBQX)-mediated synaptic responses did not differ between brevican-null and control mice (Fig. 4A). There was also no obvious difference in the voltage dependence or conductance of NMDA receptor-mediated currents, measured in the presence of picrotoxin and NBQX, between brevican-deficient and control mice (Fig. 4B). Furthermore, no significant difference in paired-pulse facilitation of the Schaffer collateral–pyramidal-cell synapses was detected by using whole-cell recordings and ISI ranging from 50 to 200 ms (Fig. 4C). This paired-pulse facilitation is a form of short-term synaptic plasticity thought to be due mainly to presynaptic mechanisms.

Next, we investigated inhibitory synaptic transmission in the presence of NBQX and CPP to prevent interference from excitatory synaptic transmission. We found no significant difference in paired-pulse depression at inhibitory synapses to pyramidal cells in the hippocampal CA1 region between mutant and control mice (Fig. 4D).

In another set of experiments, we compared sIPSCs recorded from CA1 pyramidal cells (clamped at −70 mV) in hippocampal slices from brevican-null and control mice. The averaged rise and decay times and the averaged amplitudes of the sIPSCs (40.4 ± 3.9 pA [$n = 8$] versus 37.2 ± 2.2 pA [$n = 6$]) did not differ between brevican-null and control mice (Fig.

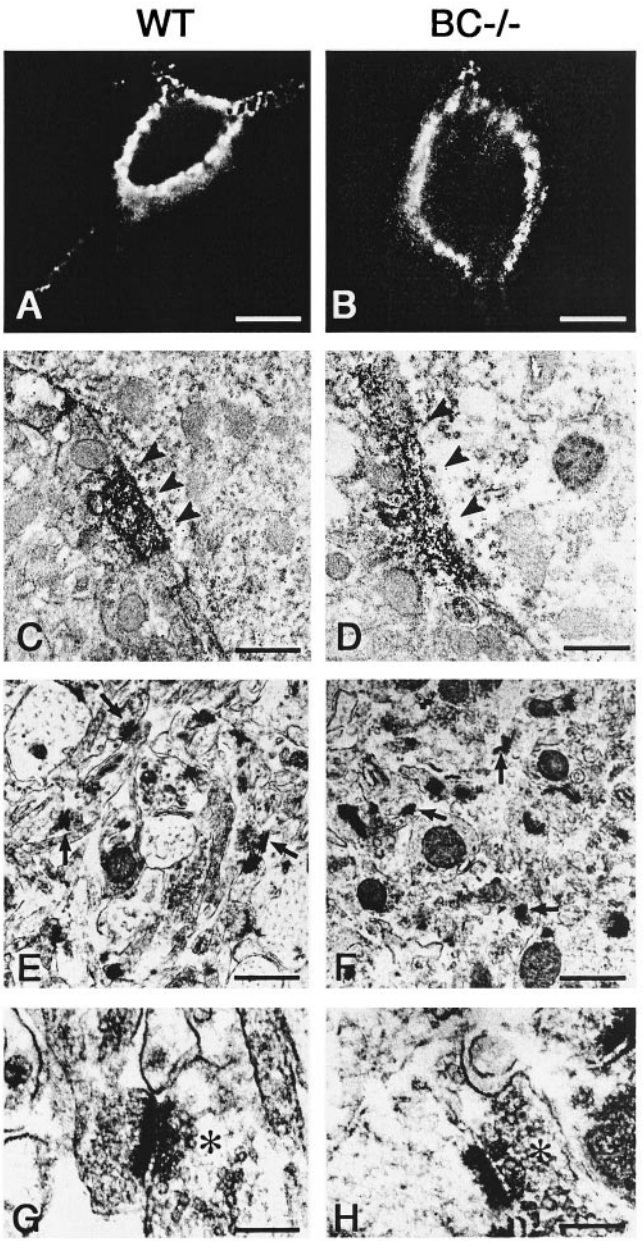

FIG. 3. Changes in PNNs but not in synapse distribution, frequency, or morphology in brevican-null mice. We performed comparative analysis of the morphology of PNNs (A through D) and of the frequency and morphology of excitatory synapses (E through H) in the hippocampi of wild-type (WT) (A, C, E, and G) and brevican knockout ($BC^{-/-}$) (B, D, F, and H) mice. As shown by immunofluorescence staining with the lectin *W. floribunda* agglutinin, PNNs are present around hippocampal nonpyramidal neurons in both WT and $BC^{-/-}$ mice (A and B). In the mutants, however, the nets appear fuzzier and are less pronounced and less concentrated close to the plasma membrane. This is confirmed by electron microscopic examination of the PNN (C and D). Arrowheads in panels C and D point to extracellular accumulations of lectin binding sites which look very structured and dense in WT mice (C) but unorganized and sparse in the brevican mutant (D). Ultrastructural examination of the distribution, frequency, and morphology of excitatory type II synapses reveals no differences between the two mouse strains (E through H). Arrows in panels E and F mark some selected synapses. Asterisks in panels G and H decorate the vesicle-filled presynaptic terminals. Bars, 10 μm (A and B), 0.5 μm (C and D), 0.8 μm (E and F), and 0.2 μm (G and H).

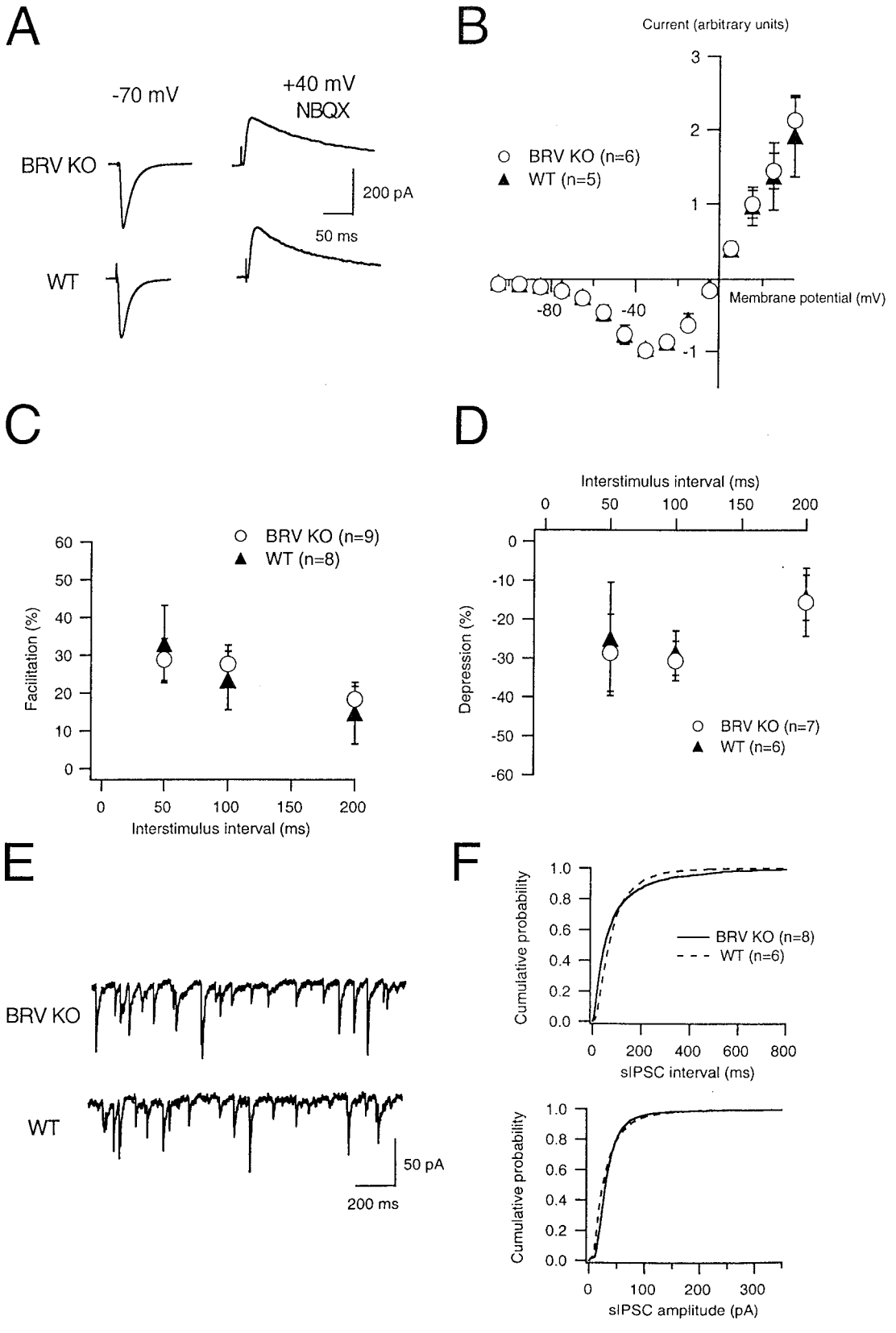

FIG. 4. Basal properties of Schaffer collateral–CA1 pyramidal-cell synapses and inhibitory interneurons. CA1 pyramidal-cell synapses are not altered in brevican-null mice. (A) Averaged excitatory postsynaptic currents (10 traces) recorded in a CA1 pyramidal cell from a brevican-deficient (BRV KO) mouse (top) or a wild-type (WT) mouse (bottom) clamped at −70 mV and at +40 mV with 5 μM NBQX in the perfusion solution. (B) Synaptically evoked NMDA receptor-mediated currents (± SEM) in CA1 pyramidal cells versus the voltage command. To block AMPA-

4E). The frequencies of sIPSCs in brevican-null versus control mice also did not differ significantly (13.9 ± 3.0 Hz [$n = 8$] versus 12.3 ± 1.6 Hz [$n = 6$]). No difference was found in the cumulative probability of the sIPSC interval or the sIPSC amplitude (Fig. 4F).

LTP of Schaffer collateral–CA1 pyramidal-cell synapses. To investigate changes in synaptic plasticity associated with the absence of brevican, we analyzed the LTP behavior of synapses between the Schaffer collaterals and principal pyramidal neurons of the CA1 region in hippocampal slice preparations. Tetanic stimulation of the Schaffer collaterals resulted in robust LTP in normal mice. Brevican-deficient mice, however, showed dramatic impairment of LTP maintenance (Fig. 5A). Although the initial peaks of the potentiation were similar for mutant and control mice, the fEPSP slope decreased rapidly in homozygous mutants, reaching levels close to baseline after about 60 min. In brain slices from wild-type mice, the potentiation was maintained for at least 180 min.

To distinguish whether the observed defect in the LTP maintenance of mutant mice is an acute effect or the result of impaired synapse development, hippocampal brain slices from rats were treated for 30 min before tetanic stimulation with antibodies against brevican. As in brevican-deficient mice, the initial excitation was still normal while the maintenance of LTP was severely impaired (Fig. 5B), indicating that the function of brevican in long-term synaptic plasticity can be acutely blocked. Control slices treated with a normal rabbit IgG fraction at the same concentration showed no difference from untreated control slices with regard to induction and maintenance of the LTP.

Normal behavior and spatial memory of brevican mutant mice. The general behavior and neurological state of brevican-deficient animals showed no obvious differences from those of their wild-type littermates with respect to gross sensory functions, reflexes, home cage activity, and food consumption. A significant increase was detected in the maximum forelimb grip strength of brevican-deficient mice (200 ± 25 p) over that of their wild-type littermates (168 ± 24 p; $F = 8.770$; $P = 0.0080$). Assessment of motor coordination by the rota-rod test revealed no differences between brevican-deficient and wild-type mice. In the open-field test, brevican-deficient mice showed behavior similar to that of their littermates, with a pronounced preference for the area closer to the walls. Exploration patterns and path lengths showed no significant differences between the two groups. Similarly, behavior in the four-hole-board test revealed no differences between mutant and control animals. On the elevated plus maze, brevican-deficient mice and wild-type controls spent similar amounts of time in the closed arms. In contrast to their wild-type littermates, brevican-deficient mice showed a preference for the open arm, which did not reach significance, on the elevated plus maze and spent less time in the center of the maze ($F = 4.747$; $P = 0.0446$). It is noteworthy that in the light-dark avoidance test, brevican-deficient mice displayed a greater tendency to stay in the illuminated area than their littermates; however, the difference did not reach significance.

In the hidden-platform Morris water maze, brevican-deficient and wild-type mice showed similar swim path lengths and escape latencies during the acquisition and reversal days. During the first probe trial, learning precision, evaluated by the number of crossings over the old platform location versus two virtual platform positions, indicated a clear preference for the old platform position among wild-type but not brevican-deficient mice. In the shuttle box paradigm, brevican-deficient mice learned the active-avoidance task. Although the level of avoidance reactions was lower for brevican-deficient mice than for their littermates at all test days (58 and 71%, respectively, at day 5), this difference did not reach significance (Fig. 6).

DISCUSSION

Brevican expression starts during late embryonic development and continues through adulthood (16, 26). An important structural role for brevican has been suggested based on its interaction with tenascin R and its presence in PNNs (9). Furthermore, in vivo experiments demonstrating modulation of glioma cell invasiveness by a brevican fragment have indicated a modulating role in cell migration (25). Since full-length brevican had no effect, the processing of brevican seemed to be important for the regulation of glioma cell migration.

Analysis of brevican-null mice demonstrated that brevican is not essential for normal brain morphology and many aspects of behavior, although alterations in protein expression and LTP maintenance were observed. Whether this relatively subtle phenotype is due to functional compensation by other lectican family members is not entirely clear. The up-regulation of neurocan, as detected by Western blot analysis of total-brain lysates, suggests a partial compensation for loss of brevican function by newly produced neurocan. However, the expression of neurocan in the cerebellum was not increased, despite high levels of brevican in the molecular and especially the granular layers of normal mice. Double knockouts of brevican and neurocan will reveal redundant functions of these molecules.

Tenascin R, which in vitro interacts strongly with brevican (1), showed normal expression in the cerebella of mutant mice. Apparently, the interaction with brevican is not important for its normal recruitment and deposition in the granular and molecular layers. Immunofluorescence suggested that deposition of tenascin C in the cerebellum might be altered. However, more-quantitative techniques have to be used to test this possibility. Brevican is found in PNNs together with other

receptor-mediated currents, 5 μM NBQX was added to the aCSF. In each experiment the currents were normalized to the maximum inward current obtained in that experiment. (C) Averaged paired-pulse facilitation (± SEM) of excitatory postsynaptic currents at different ISI in Schaffer collateral–CA1 pyramidal-cell synapses from brevican-null (open circles) and wild-type (filled triangles) mice. (D) Averaged paired-pulse depression (± SEM) of evoked IPSCs at different ISI in CA1 pyramidal cells from brevican-null (open circles) and wild-type (filled triangles) mice. (E) Recordings of sIPSCs from a CA1 pyramidal cell elicited in a hippocampal slice from a brevican-null (top trace) and a wild-type (bottom trace) mouse. (F) Cumulative probabilities for sIPSC intervals (top graph) and amplitudes (bottom graph) in CA1 pyramidal cells in hippocampal slices from brevican-deficient (solid lines) or wild-type (dashed lines) mice.

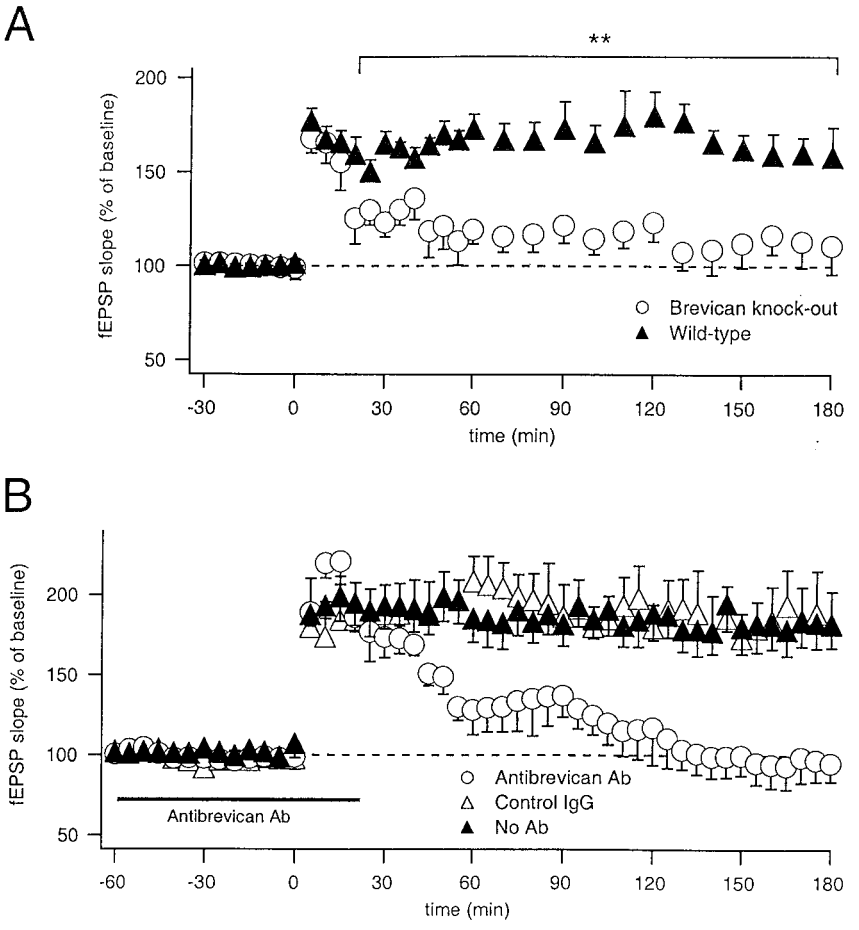

FIG. 5. Impaired maintenance of LTP in hippocampal slices from brevican-deficient mice and from normal rats treated with antibodies (Ab) against brevican. (A) Time course of LTP in Schaffer collateral–CA1 cell synapses from brevican-null mice (open circles) and wild-type controls (filled triangles). LTPs were induced by tetanizing the Schaffer collaterals with three 50-impulse trains (100 Hz), with a 5-min interval between trains ($t = 0$ min). Presented is the averaged fEPSP slope ± SEM. (B) Time course of LTP in Schaffer collateral–CA1 cell synapses in hippocampal slices from wild-type rats either treated with rabbit anti-brevican IgG (open circles) or with normal rabbit IgG (open triangles) or left untreated (filled triangles). LTPs were induced as described above. Note that anti-brevican IgG leads to a clear decrease in LTP maintenance, which is not observed with the control IgG.

molecules such as tenascin R, neurocan, and hyaluronan (9). These networks can also form in the absence of brevican, although their structure might be different, as indicated by the slightly altered staining with *W. floribunda* agglutinin. This is in accordance with the observation of Bruckner et al. (3) that in mice lacking the brevican binding partner tenascin R, the PNNs show a structurally changed appearance. Moreover, in the brains of these mice, the PNNs contain less brevican immunoreactivity than those of wild-type mice. PNNs have been suggested to isolate and stabilize existing synapses and to prevent the formation of new synaptic contacts (43). However, no increase in synapse density was detected in the hippocampi of brevican-deficient mice. It is possible that brevican contributes to another, yet unknown function of PNNs.

In testing brain functions by use of established electrophysiological paradigms for brain sections, we observed a severe defect in the maintenance of LTP in brain slices of mutant mice, although the initial fEPSP slope was normal. Surprisingly, neither excitatory transmission via AMPA and NMDA receptors nor inhibitory synaptic transmission via GABA(A) receptors showed any abnormal characteristics in brevican-null mice. Furthermore, short-term plasticity, as measured by paired-pulse facilitation of excitatory synaptic transmission or paired-pulse depression of inhibitory synaptic transmission onto CA1 pyramidal cells, was similar in mutant and control mice, suggesting a complex cause for the observed LTP defect.

Brevican is found between synapses close to the neuronal membrane. Besides preventing the formation of new synapses, it has been speculated that brevican might function as an insulator, sealing the synapses and preventing loss of transmitter substances from the synaptic cleft to the periphery (42). The efficacy of the synaptic cross talk might be dependent on the extracellular space surrounding the synapses, i.e., on intersynaptic geometry and diffusion parameters (37). This would suggest a mainly structural role for brevican at this location. Since treatment of brain slices of normal rats with antibodies against brevican results in acute impairment of LTP maintenance, this hypothesis seems less likely. Such acute inhibition by antibodies is more charac-

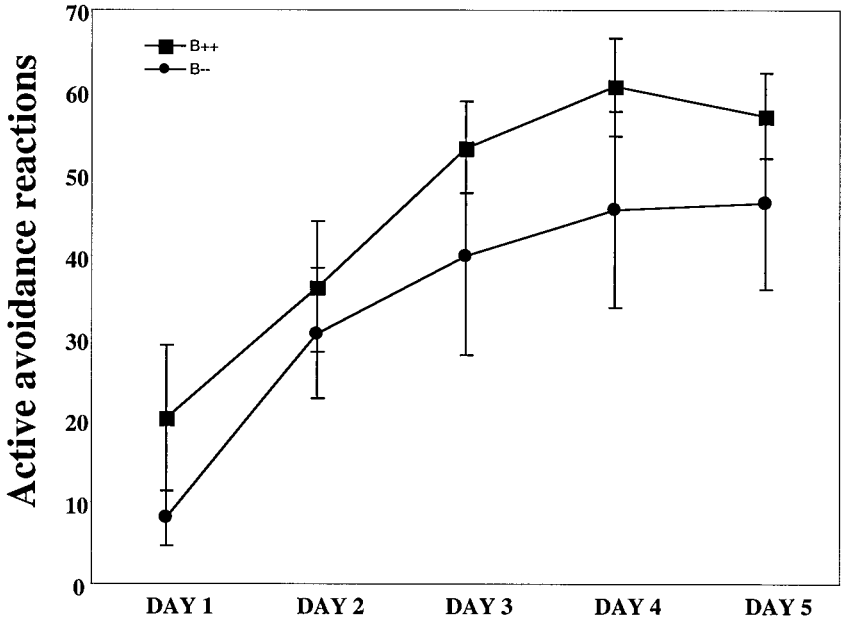

FIG. 6. Performance of brevican-deficient mice and their wild-type littermates in the shuttle box. Brevican-deficient mice (filled circles) (n = 8) and their wild-type littermates (filled squares) (n = 8) were subjected to 80 trials per day over 5 days. The number of active-avoidance reactions ± SEM for the mutants was slightly, but not significantly, lower on all test days.

teristic for interference with signal transduction processes. It has been shown that secreted brevican can bind to cell surface sulfatides and SGGLs (18). Blocking these interactions might cause changes in signal transduction, which eventually result in the LTP defect. It has recently been shown that the interaction between the lectin domain of brevican and cell surface SGGLs promotes neuronal adhesion and neurite outgrowth (18). Furthermore, brevican exists in a glycosylphosphatidylinositol-anchored form also (33). Since several glypiated cell surface molecules are known to be signal transducers, the binding of antibodies might affect the physiological status within the cell (12). A further hypothetical explanation for the reduced LTP maintenance could be the role of ECM components as low-affinity receptors and local traps for growth factors and cytokines (for a review, see reference 32) which are known to strongly influence LTP duration (10). Defects in LTP sometimes, but not always, correspond to defects in learning and memory (21). However, using two different models for learning and memory, we could not observe a significant difference between mutant and wild-type mice. Brevican-deficient mice displayed generally normal acquisition of the task in the water maze, indicating that spatial learning is not generally disturbed. Yet the reduced platform preference in the first probe trial could indicate subtle alterations in memory consolidation. Further studies are required to address this in more detail. In agreement with grossly normal hippocampal functions, acquisition and performance level were only slightly, not significantly, reduced in the two-way active-avoidance paradigm. Other behavioral paradigms also failed to reveal a significant defect in brevican-null mice. In particular, motor coordination as addressed in the rota-rod test, which reflects cerebellar functions, was strikingly normal.

Intact learning in the absence of LTP has also been observed previously. For example, antisense knockdown of the potassium channel Kv1.4 (14), targeted disruption of the AMPA receptor (44), Thy-1 knockout (23), overexpression of NR2D, a predominantly embryonic NMDA receptor subunit (27), and brain-derived neurotrophic factor (BDNF) heterozygotes (19) all resulted in absent or reduced LTP but did not change spatial memory. It seems that some of the molecular defects that cause LTP impairment also cause learning deficits in parallel but that the LTP impairment itself is not directly connected to learning. Currently, it is not clear whether there is a common in vivo consequence in all cases where an LTP defect is observed in vitro.

It has been shown previously that lecticans and lectican-interacting proteins are involved in LTP formation and maintenance. It was recently reported that mice lacking a functional neurocan gene have reduced maintenance of late-phase LTP (45). The LTP defect observed in brevican-deficient mice is much more pronounced. Furthermore, despite the structural similarity and perhaps similar functional roles in the maintenance of LTP, loss of brevican cannot be fully compensated for by neurocan, and vice versa. Both effects could be due to the fact that in the brains of adult mice large amounts of brevican but only small amounts of neurocan are present, while the relation is the opposite during embryonic development. Targeted inactivation of the gene for tenascin R, which binds to all lecticans but most strongly to brevican, resulted in a 50%-reduced LTP (31). In contrast to the brevican knockout mice, tenascin R-deficient mice also showed increased excitatory transmission and reduced perisomatic inhibition. As in brevican-null mice, paired-pulse facilitation was normal in tenascin R-deficient mice. In addition it was found that treatment of brain slices with antibodies against HNK-1, a carbohydrate epitope expressed on many neuronal cell surface molecules such as the brevican

binding SGGLs and on tenascin R, increased LTP. Treatment with antibodies against HNK-1 did not change the defective LTP observed with hippocampal slices from tenascin R-deficient mice, suggesting a crucial role for the HNK-1 carbohydrate of tenascin R (36). Finally, treatment of hippocampal slices with chondroitinase ABC, which removes chondroitin sulfate side chains of brevican and other molecules, led to a 50% reduction in LTP (4). These data indicate crucial roles of proteoglycans and proteoglycan binding molecules in the formation and modulation of LTP, although the underlying molecular mechanism of these different LTP defects is not clear. The efficacy of the synaptic cross talk might be dependent on the extracellular space surrounding the synapses, i.e., on intersynaptic geometry and diffusion parameters (37). This suggests an important role for proteoglycans present in the vicinity of synapses, which could contribute to diffusion barriers in the extracellular space.

ACKNOWLEDGMENTS

We thank A. Lundquist and M. Marunde for expert technical help. We are grateful to K. Sowa for expert technical help with the behavioral experiments. We thank R. Timpl and A. Aspberg for antibodies used in this study.

This work was carried out with the support of the Swedish National Research Foundation and the SSF inflammation program and by grants from the DFG (Se 952/2-1 and -2-2), Land Sachsen-Anhalt (LSA 3004A/0088H), and Fonds der Chemischen Industrie.

REFERENCES

1. **Aspberg, A., R. Miura, S. Bourdoulous, M. Shimonaka, D. Heinegard, M. Schachner, E. Ruoslahti, and Y. Yamaguchi.** 1997. The C-type lectin domains of lecticans, a family of aggregating chondroitin sulfate proteoglycans, bind tenascin-R by protein-protein interactions independent of carbohydrate moiety. Proc. Natl. Acad. Sci. USA **94:**10116–10121.
2. **Auffray, C., and F. Rougeon.** 1980. Purification of mouse immunoglobulin heavy-chain messenger RNAs from total myeloma tumor RNA. Eur. J. Biochem. **107:**303–314.
3. **Bruckner, G., J. Grosche, S. Schmidt, W. Hartig, R. U. Margolis, B. Delpech, C. I. Seidenbecher, R. Czaniera, and M. Schachner.** 2000. Postnatal development of perineuronal nets in wild-type mice and in a mutant deficient in tenascin-R. J. Comp. Neurol. **428:**616–629.
4. **Bukalo, O., M. Schachner, and A. Dityatev.** 2001. Modification of extracellular matrix by enzymatic removal of chondroitin sulfate and by lack of tenascin-R differentially affects several forms of synaptic plasticity in the hippocampus. Neuroscience **104:**359–369.
5. **Crawley, J. N.** 1981. Neuropharmacologic specificity of a simple animal model for the behavioral actions of benzodiazepines. Pharm. Biochem. Beh. **15:**695–699.
6. **Crawley, J. N., and F. K. Goodwin.** 1980. Preliminary report of a simple animal behavior model for the anxiolytic effects of benzodiazepines. Pharm. Biochem. Beh. **13:**167–170.
7. **Fässler, R., and M. Meyer.** 1995. Consequences of lack of β1 integrin gene expression in mice. Genes Dev. **9:**1896–1908.
8. **Grumet, M., P. Milev, T. Sakurai, L. Karthikeyan, M. Bourdon, R. K. Margolis, and R. U. Margolis.** 1994. Interactions with tenascin and differential effects on cell adhesion of neurocan and phosphacan, two major chondroitin sulfate proteoglycans of nervous tissue. J. Biol. Chem. **269:**12142–12146.
9. **Hagihara, K., R. Miura, R. Kosaki, E. Berglund, B. Ranscht, and Y. Yamaguchi.** 1999. Immunohistochemical evidence for the brevican–tenascin-R interaction: colocalization in perineuronal nets suggests a physiological role for the interaction in the adult rat brain. J. Comp. Neurol. **410:**256–264.
10. **Jankowsky, J. L., and P. H. Patterson.** 1999. Cytokine and growth factor involvement in long-term potentiation. Mol. Cell. Neurosci. **14:**273–286.
11. **Jones, B. J., and D. J. Roberts.** 1968. The quantitative measurement of motor inco-ordination in naive mice using an accelerating rota-rod. J. Pharm. Pharmacol. **20:**302–304.
12. **Kasahara, K., and Y. Sanai.** 2000. Functional roles of glycosphingolipids in signal transduction via lipid rafts. Glycoconj. J. **17:**153–162.
13. **Lister, R. G.** 1987. The use of a plus-maze to measure anxiety in the mouse. Psychopharmacology **92:**180–185.
14. **Meiri, N., M. K. Sun, Z. Segal, and D. L. Alkon.** 1998. Memory and long-term potentiation (LTP) dissociated: normal spatial memory despite CA1 LTP elimination with Kv1.4 antisense. Proc. Natl. Acad. Sci. USA **95:**15037–15042.
15. **Meyer, O. A., H. A. Tilson, W. C. Byrd, and M. T. Riley.** 1979. A method for the routine assessment of fore- and hindlimb grip strength of rats and mice. Neurobehav. Toxicol. **1:**233–236.
16. **Milev, P., P. Maurel, A. Chiba, M. Mevissen, S. Popp, Y. Yamaguchi, R. K. Margolis, and R. U. Margolis.** 1998. Differential regulation of expression of hyaluronan-binding proteoglycans in developing brain: aggrecan, versican, neurocan, and brevican. Biochem. Biophys. Res. Commun. **247:**207–212.
17. **Miura, R., A. Aspberg, I. M. Ethell, K. Hagihara, R. L. Schnaar, E. Ruoslahti, and Y. Yamaguchi.** 1999. The proteoglycan lectin domain binds sulfated cell surface glycolipids and promotes cell adhesion. J. Biol. Chem. **274:**11431–11438.
18. **Miura, R., I. M. Ethell, and Y. Yamaguchi.** 2001. Carbohydrate-protein interactions between HNK-1-reactive sulfoglucuronyl glycolipids and the proteoglycan lectin domain mediate neuronal cell adhesion and neurite outgrowth. J. Neurochem. **76:**413–424.
19. **Montkowski, A., and F. Holsboer.** 1997. Intact spatial learning and memory in transgenic mice with reduced BDNF. Neuroreport **8:**779–782.
20. **Morris, R. G. M.** 1984. Development of a water-maze procedure for studying spatial learning in the rat. J. Neurosci. Methods **11:**47–60.
21. **Moser, M. B., and E. I. Moser.** 2000. Pretraining and the function of hippocampal long-term potentiation. Neuron **26:**559–561.
22. **Niederost, B. P., D. R. Zimmermann, M. E. Schwab, and C. E. Bandtlow.** 1999. Bovine CNS myelin contains neurite growth-inhibitory activity associated with chondroitin sulfate proteoglycans. J. Neurosci. **19:**8979–8989.
23. **Nosten-Bertrand, M., M. L. Errington, K. P. Murphy, Y. Tokugawa, E. Barboni, E. Kozlova, D. Michalovich, R. G. Morris, J. Silver, C. L. Stewart, T. V. Bliss, and R. J. Morris.** 1996. Normal spatial learning despite regional inhibition of LTP in mice lacking Thy-1. Nature **379:**826–829.
24. **Novak, U., and A. H. Kaye.** 2000. Extracellular matrix and the brain: components and function. J. Clin. Neurosci. **4:**280–290.
25. **Nutt, C. L., C. A. Zerillo, G. M. Kelly, and S. Hockfield.** 2001. Brain enriched hyaluronan binding (BEHAB)/brevican increases aggressiveness of CNS-1 gliomas in Lewis rats. Cancer Res. **61:**7056–7059.
26. **Ogawa, T., K. Hagihara, M. Suzuki, and Y. Yamaguchi.** 2001. Brevican in the developing hippocampal fimbria: differential expression in myelinating oligodendrocytes and adult astrocytes suggests a dual role for brevican in central nervous system fiber tract development. J. Comp. Neurol. **432:**285–295.
27. **Okabe, S., C. Collin, J. M. Auerbach, N. Meiri, J. Bengzon, M. B. Kennedy, M. Segal, and R. D. McKay.** 1998. Hippocampal synaptic plasticity in mice overexpressing an embryonic subunit of the NMDA receptor. J. Neurosci. **18:**4177–4188.
28. **Pellow, S., P. Chopin, S. E. File, and M. Briley.** 1985. Validation of open: closed arm entries in an elevated plus-maze as a measure of anxiety in the rat. J. Neurosci. Methods **14:**149–167.
29. **Rauch, U., H. Meyer, C. Brakebusch, C. Seidenbecher, E. D. Gundelfinger, D. R. Beier, and R. Fässler.** 1997. Sequence and chromosomal localization of the mouse brevican gene. Genomics **44:**15–21.
30. **Rogers, D. C., E. M. Fisher, S. D. Brown, J. Peters, A. J. Hunter, and J. E. Martin.** 1997. Behavioral and functional analysis of mouse phenotype: SHIRPA, a proposed protocol for comprehensive phenotype assessment. Mamm. Genome **8:**711–713.
31. **Saghatelyan, A. K., A. Dityatev, S. Schmidt, T. Schuster, U. Bartsch, and M. Schachner.** 2001. Reduced perisomatic inhibition, increased excitatory transmission, and impaired long-term potentiation in mice deficient for the extracellular matrix glycoprotein tenascin-R. Mol. Cell. Neurosci. **17:**226–240.
32. **Schlessinger, J., I. Lax, and M. Lemmon.** 1995. Regulation of growth factor activation by proteoglycans: what is the role of the low affinity receptors? Cell **83:**357–360.
33. **Seidenbecher, C. I., K. Richter, U. Rauch, R. Fässler, C. C. Garner, and E. D. Gundelfinger.** 1995. Brevican, a chondroitin sulfate proteoglycan of rat brain, occurs as secreted and cell surface glycosylphosphatidylinositol-anchored isoforms. J. Biol. Chem. **270:**27206–27212.
34. **Smalla, K. H., H. Matthies, K. Langnase, S. Shabir, T. M. Bockers, U. Wyneken, S. Staak, M. Krug, P. W. Beesley, and E. D. Gundelfinger.** 2000. The synaptic glycoprotein neuroplastin is involved in long-term potentiation at hippocampal CA1 synapses. Proc. Natl. Acad. Sci. USA. **97:**4327–4332.
35. **Stork, O., H. Welzl, C. T. Wotjak, D. Hoyer, M. Delling, H. Cremer, and M. Schachner.** 1999. Anxiety and increased 5-HT1A receptor response in NCAM null mutant mice. J. Neurobiol. **40:**343–355.
36. **Strekalova, T., C. T. Wotjak, and M. Schachner.** 2001. Intrahippocampal administration of an antibody against the HNK-1 carbohydrate impairs memory consolidation in an inhibitory learning task in mice. Mol. Cell. Neurosci. **17:**1102–1113.
37. **Sykova, E.** 2001. Glial diffusion barriers during aging and pathological states. Prog. Brain Res. **132:**339–363.

38. **Tisay, K. T., and B. Key.** 1999. The extracellular matrix modulates olfactory neurite outgrowth on ensheathing cells. J. Neurosci. **19:**9890–9899.
39. **Wishaw, I. Q., F. Haun, and B. Kolb.** 1999. Analysis of behavior in laboratory rodents, p. 1243–1275. *In* U. Windhorst and H. Johansson (ed.), Modern techniques in neuroscience. Springer, Berlin, Germany.
40. **Wolfer, D., and H.-P. Lipp.** 1992. A computer program for detailed off-line analysis of Morris water maze behavior. J. Neurosci. Methods **41:**65–74.
41. **Wright, J. W., E. A. Kramar, S. E. Meighan, and J. W. Harding.** 2002. Extracellular matrix molecules, long-term potentiation, memory consolidation and the brain angiotensin system. Peptides **23:**221–246.
42. **Yamada, H., B. Fredette, K. Shitara, K. Hagihara, R. Miura, B. Ranscht, W. B. Stallcup, and Y. Yamaguchi.** 1997. The brain chondroitin sulfate proteoglycan brevican associates with astrocytes ensheathing cerebellar glomeruli and inhibits neurite outgrowth from granule neurons. J. Neurosci. **17:**7784–7795.
43. **Yamaguchi, Y.** 2000. Lecticans: organizers of the brain extracellular matrix. Cell. Mol. Life Sci. **57:**276–289.
44. **Zamanillo, D., R. Sprengel, O. Hvalby, V. Jensen, N. Burnashev, A. Rozov, K. M. Kaiser, H. J. Koster, T. Borchardt, P. Worley, J. Lubke, M. Frotscher, P. H. Kelly, B. Sommer, P. Andersen, P. H. Seeburg, and B. Sakmann.** 1999. Importance of AMPA receptors for hippocampal synaptic plasticity but not for spatial learning. Science **284:**1805–1811.
45. **Zhou, X. H., C. Brakebusch, H. Matthies, T. Oohashi, E. Hirsch, M. Moser, M. Krug, C. I. Seidenbecher, T. M. Boeckers, U. Rauch, R. Buettner, E. D. Gundelfinger, and R. Fässler.** 2001. Neurocan is dispensable for brain development. Mol. Cell. Biol. **21:**5970–5978.